Organic & Biomolecular Chemistry

PAPER

View Article Online
View Journal

Cite this: DOI: 10.1039/c5ob01082a

Pyrido[1,2-*a*]pyrimidinium ions – a novel bridgehead nitrogen heterocycles: synthesis, characterisation, and elucidation of DNA binding and cell imaging properties†

Susanta Kumar Manna,*[a] Arabinda Mandal,[a] Suresh Kumar Mondal,[a] Arup Kr Adak,[a] Akash Jana,[a] Somnath Das,[b] Sourav Chattopadhyay,[c] Somenath Roy,[c] Shyamal Kr Ghorai,[d] Shubhankar Samanta,*[a] Maidul Hossain*[b] and Mahiuddin Baidya*[e]

Received 28th May 2015,
Accepted 19th June 2015

DOI: 10.1039/c5ob01082a

www.rsc.org/obc

A novel class of bridgehead nitrogen heterocycles, pyrido[1,2-*a*]pyrimidinium ions, has been readily synthesized by a two-step one-pot reaction in high yields (up to 93%). These ionic compounds are bench stable and moisture tolerant and have highly fluorescent properties (quantum yield up to 0.65). A characteristic bright bluish fluorescence was observed in polar solvents such as acetonitrile and fluorescent intensity gradually diminishes with decreasing the polarity of the medium, which becomes almost negligible in toluene. These compounds also show interesting bioactivity. DNA interaction, imaging, and viability experiments with human leukemic Jurkat and KG-1A cells revealed that they are potential candidates for cancer diagnosis.

Introduction

Nitrogen fused heterocyclic molecular frameworks constitute a very rapidly developing field of research due to their presence in numerous naturally occurring compounds, their widespread application in organic synthesis, and their diverse biological activities.[1] Particularly the bridgehead nitrogen heterocycles, for instance imidazo[1,2-*a*]pyridine, pyrido[1,2-*a*]pyrimidine, pyrazolopyrimidine *etc.*, are very popular with characteristic pharmacological properties such as antiviral, analgesic, antiallergic, antiasthmatic, antipsychotic activities *etc.* (Scheme 1a).[2–5] These privileged structural motifs and derivatives thereof are also synthetically appealing and have remained in the focus of interest.[6] Often they are used as the intermediates in the synthesis of drug candidates.[3,7] While the synthesis of various bicyclic bridgehead nitrogen heterocycles is well established, synthetic protocols of their polycyclic analogues having tetracyclic and tricyclic cores are more challenging and are very limited in the literature.[6c,8] Recently, we developed novel syntheses of polycyclic bridgehead benzimidazole and pyrrolo[1,2-*b*]pyrazolone derivatives (Scheme 1b).[9] Herein, we have reported the one pot synthesis of brand new polycyclic fused pyrido[1,2-*a*]pyrimidinium ions (Scheme 1c).

These compounds are not only ionic but also show a highly conjugated π-electron system. Hence, we anticipated their interaction with cellular DNA.[10] Furthermore, these compounds are highly fluorescent and will allow visual imaging of living cells with ease. Thus, in parallel with their synthesis, we have also studied the cell imaging and viability of human leukemic Jurkat and KG-1A cells with this new class of bridgehead nitrogen heterocycles. We have evaluated the binding affinity and stoichiometry of the synthesized heterocycles to bind calf-thymus DNA (CT-DNA) by UV-Vis and fluorescence spectroscopic titration. The thermodynamic changes associated with the binding are also characterized through isothermal titration calorimetry (ITC). These findings will have direct implications in cancer diagnosis.[11]

[a]*Department of Chemistry, Haldia Government College, Haldia 721657, India. E-mail: smanna19@gmail.com, mbaidya@iitm.ac.in, hossainm@mail.vidyasagar.ac.in*
[b]*Department of Chemistry and Chemical Technology, Vidyasagar University, Midnapore 721102, India*
[c]*Department of Human Physiology with Community Health, Vidyasagar University, Midnapore 721102, India*
[d]*Department of Chemistry and Biochemistry, Presidency University, 86/1, College Street, Kolkata 700073, India*
[e]*Department of Chemistry, Indian Institute of Technology Madras, Chennai 600036, India*

† Electronic supplementary information (ESI) available. CCDC 1403910. For ESI and crystallographic data in CIF or other electronic format see DOI: 10.1039/c5ob01082a

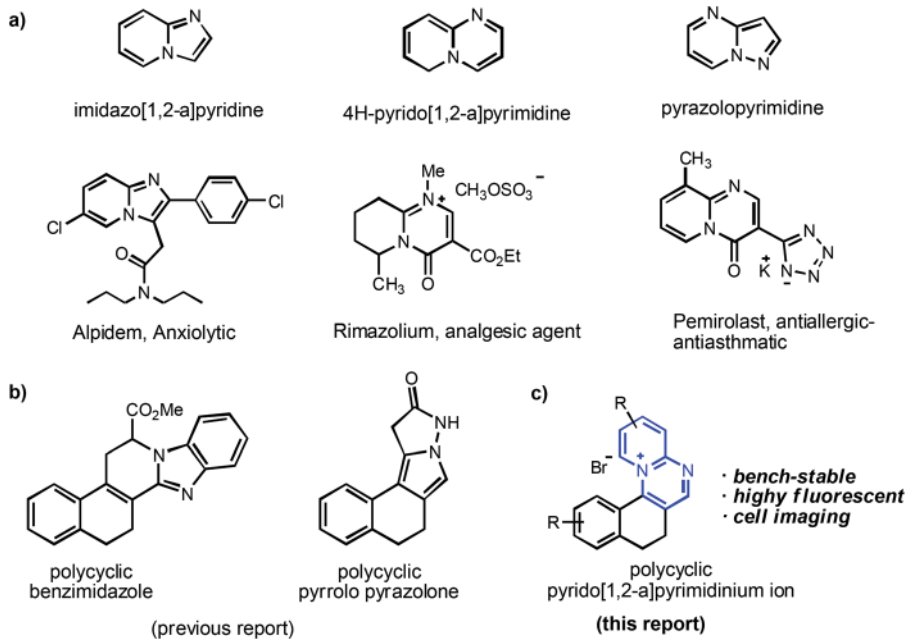

Scheme 1 Common nitrogen bridgehead heterocycles and bioactive compounds (a), polycyclic nitrogen bridgehead heterocycles (b), and brand new pyridopyrimidinium ions (c).

Results and discussion

Synthesis of pyrido[1,2-*a*]pyrimidinium ions

We commenced the synthesis with readily available β-bromovinyl aldehyde **1a**.[12] Upon refluxing with commercially available 2-aminopyridine in dichloromethane in the presence of catalytic amounts of acetic acid, **1a** smoothly delivered the desired tetracyclic product **2a** in 50% isolated yield (Table 1, entry 1). The reaction did not proceed in the absence of a catalyst or at 25 °C. Changing the solvent to acetonitrile increased the yield (86%) and the best result was obtained in anhydrous methanol (91%, entry 3). Other solvents like THF and DMF are not suitable for this purpose (entries 4 and 5). The product **2a** was also crystalized and the X-ray analysis unambiguously confirmed the polycyclic ionic structure (Fig. 1).

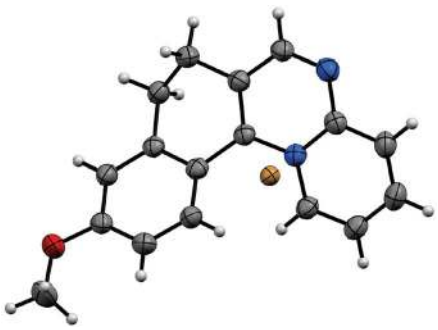

Fig. 1 Crystal structure of **2a** (ORTEP view).

Table 1 Synthesis of polycyclic pyrido[1,2-*a*]pyrimidinium ions **2a**

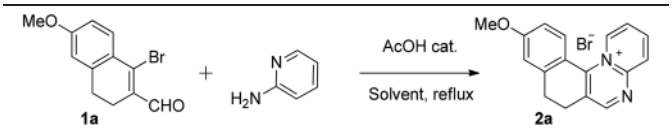

Entry	Solvent	Time (h)	Yield (%)
1	CH_2Cl_2	8	50
2	CH_3CN	8	86
3	MeOH	8	91
4	THF	12	Trace
5	DMF	18	Trace

Under the optimized conditions, the scope of the reaction was examined (Table 2). The reaction smoothly proceeded for a series of substituted β-bromovinyl aldehydes **1** delivering tetracyclic and tricyclic nitrogen bridgehead products (**2b–g**) substituted with both electron donating and electron withdrawing groups in very good yields. The reaction is not limited only to 2-aminopyridine. It is equally facile with other substituted 2-aminopyridines. When chloro and methyl substituted 2-aminopyridines were implemented, the desired polycyclic pyrido[1,2-*a*]pyrimidinium ions were obtained in comparable yields (**2h–s**), which further broadened our reaction scope. It is important to mention that these new compounds are bench-stable and moisture tolerant and can be easily purified by column chromatography.

Table 2 The reaction scope of the synthesis of polycyclic pyrido[1,2-*a*]pyrimidinium ions **2**

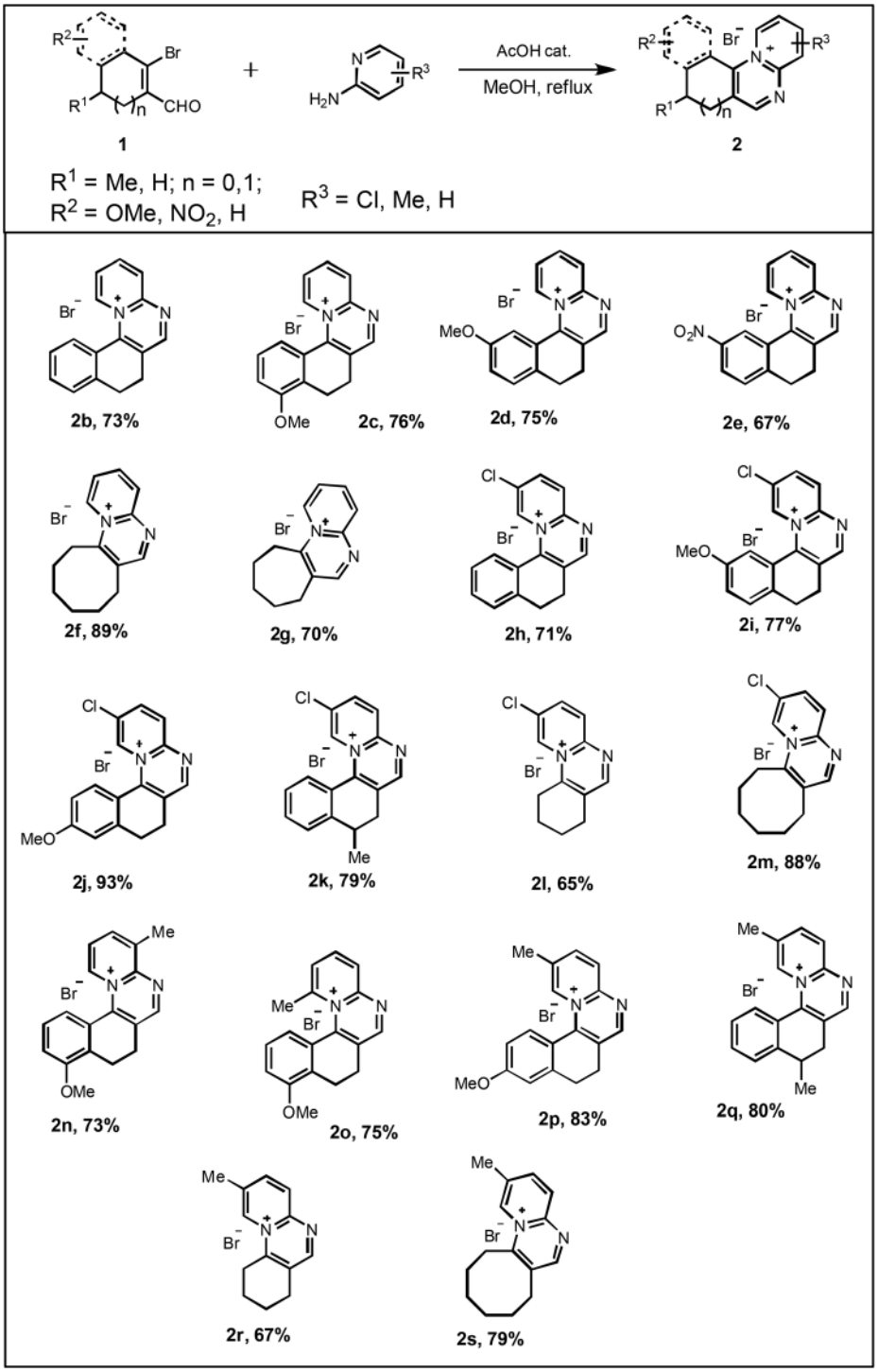

A possible reaction mechanism is shown in Scheme 2. Compound **1** gets activated in the presence of acetic acid catalyst and generates the imine **A** by condensation with 2-aminopyridine. The imine **A** undergoes a facile intramolecular 1,4-addition to produce the intermediate **B**, which on displacement of bromide ions delivers the final product **2** and regenerates acetic acid for the next cycle.

Reaction conditions

1 (1.0 mmol), substituted 2-aminopyridine (1.1 mmol), AcOH (catalytic), MeOH (3 ml), reflux, 8 hours.

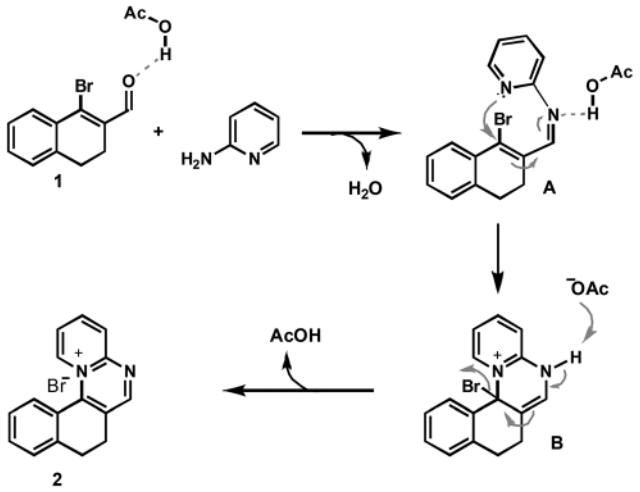

Scheme 2 Plausible mechanism for the formation of **2**.

Table 3 The data of the photophysical studies of **2a** (2×10^{-5} M) in different solvents at 298 K

Solvent	ε	λ_{max} of absorbance	λ_{max} of emission	Quantum yield (ϕ)
Water	80.1	371.0 nm	447.0 nm	0.65
Dimethylsulphoxide (DMSO)	46.7	371.0 nm	441.0 nm	0.58
Acetonitrile (ACN)	37.5	372.0 nm	442.0 nm	0.57
N,*N*-Dimethylformamide (DMF)	36.7	374.2 nm	445.8 nm	0.54
Acetone	20.7	378.0 nm	458.0 nm	0.50
Dichloromethane (DCM)	8.93	384.0 nm	462.4 nm	0.35
Tetrahydrofuran (THF)	7.58	385.0 nm	463.0 nm	0.30
Chloroform	4.81	405.3 nm	480.0 nm	0.18
Toluene	2.38	414.0 nm	486.6 nm	0.13

Photophysical studies

Interestingly, all of these polycyclic pyrido[1,2-*a*]pyrimidinium ions are highly fluorescent in nature and we were interested in investigating this property in more detail. Compound **2a** was selected as a model substrate for this purpose.

Absorption and emission spectra

The absorption spectra of **2a** in the various solvents were recorded at 298 K (Fig. 2a). We have observed that the wavelength maximum is red shifted from 371 nm to 414 nm with decreasing the solvent polarity from DMSO to toluene, although the nature of the spectrum is almost similar in all the solvents. Fig. 2b represents the emission spectra of **2a** at room temperature (298 K) in different non-polar and polar solvents (aprotic). The wavelength maxima of the emission spectra are also red shifted from 441 nm to 486.6 nm with decreasing polarity (DMSO → toluene). This indicates that the polar solvent stabilizes the ground state more than the excited state. The quantum yields of the emission of **2a** in different non-polar and polar (aprotic) solvents were calculated and Table 3 shows that the quantum yield decreases with decreasing polarity of the solvents. The emission spectra and the quantum yields of **2a** in the various solvents are well reflected in the lifetime measurements (Fig. 3). The decay of **2a** was measured by monitoring the wavelength maxima and was found to fit with double exponential. The average lifetime decreases with decreasing solvent polarity (Table 4).

We have also considered mixed solvents containing acetonitrile and toluene for this study. It has been observed that the position of the emission maxima of **2a** shifts towards longer wavelength when the composition of the mixed solvent changes from pure acetonitrile to pure toluene (Fig. 4). Consequently, the quantum yield of the emission in the acetonitrile–toluene mixed solvent decreases as a function of percent volume of toluene in the mixed solvent composition.

Biological activity studies

Cell viability. Two human leukemic cells, Jurkat and KG-1A, were seeded into 96 wells of tissue culture plates having 180 μl

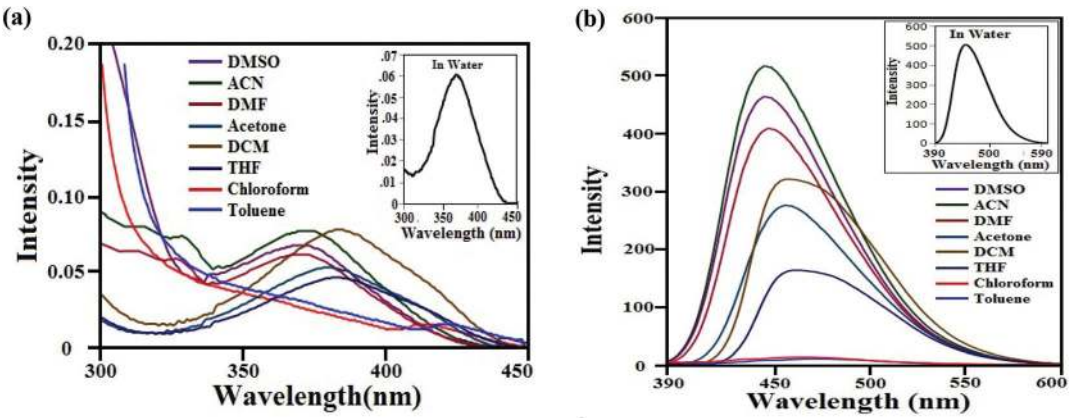

Fig. 2 Absorption spectra (a) and emission spectra (b) of **2a** (2×10^{-5} M) in various solvents at 298 K [inset: absorption spectra and emission spectra of **2a** (2×10^{-5} M) in water].

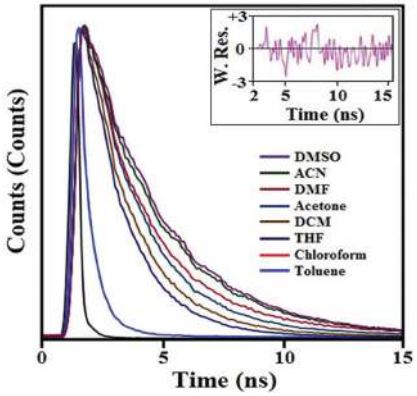

Fig. 3 Fluorescence decay of **2a** (2×10^{-5} M) monitored at the λ_{max} of emission at 298 K in various solvents.

Table 4 Lifetime of **2a** (2×10^{-5} M) monitoring the λ_{max} of emission at 298 K in various solvents

Solvent	τ_1 (ns)	τ_2 (ns)	$\langle\tau\rangle$ (ns)	χ^2
Water	4.8 (16%)	2.9 (84%)	3.16	1.03
Dimethylsulphoxide (DMSO)	4.1 (30%)	2.3 (70%)	2.84	0.99
Acetonitrile (ACN)	4.0 (25%)	2.3 (75%)	2.72	1.03
N,*N*-Dimethylformamide (DMF)	3.8 (26%)	2.1 (74%)	2.54	0.98
Acetone	3.7 (29%)	1.9 (71%)	2.42	1.10
Dichloromethane (DCM)	2.8 (38%)	1.5 (62%)	1.99	1.05
Tetrahydrofuran (THF)	2.8 (37%)	1.4 (63%)	1.92	0.95
Chloroform	1.5 (30%)	0.9 (70%)	1.08	0.90
Toluene	1.5 (28%)	0.8 (72%)	1.00	1.04

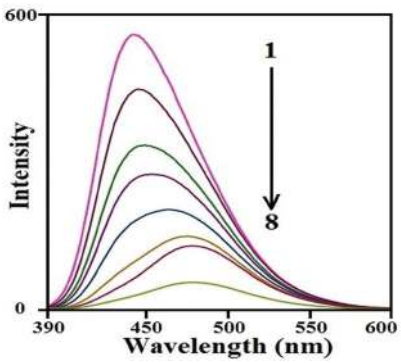

Fig. 4 Emission spectra of **2a** (2×10^{-5} M) in acetonitrile and toluene mixed solvent; curves (1–8) represent 100%, 90%, 80%, 70%, 60%, 50%, 40%, and 20% volume of acetonitrile respectively; λ_{exc} = 372 nm; excitation and emission band pass = 10 nm each.

of complete medium and were incubated for 48 h. Compound **2a** was added to the cells at different concentrations (1–25 μg ml^{-1}) and incubated for 24 h at 37 °C in a humidified incubator (NBS) maintained with 5% CO_2. The cell viability was estimated using 3-(4,5-dimethylthiazol)-2-diphenyltetrazolium bromide following the method of Chattopadhyay *et al.*[13] The pyridopyrimidinium ion **2a** exhibits promising toxicity activity against the used cells *in vitro* (Fig. 5a). It kills the leukemia cells significantly at the dose of 1, 5, 10 and 25 μg ml^{-1}. Jurkat cells were 94.26, 70.28, 42.75, 21.03%, and KG-1A cells were 93.15, 73.64, 39.98 and 23.11%, respectively. These outcomes demonstrate that cancerous white blood cells are significantly more susceptible to compound **2a**.

Lactose dehydrogenase (LDH) activity. LDH activity in serum was estimated with a sandwich ELISA kit (Tulip, Mumbai, India) and the activity of LDH was expressed as μM dl^{-1}. Fig. 5b shows that compound **2a** induced LDH activity in both Jurkat and KG-1A cells and the effect is gradually increasing with the increase of sample loading from the control level.

Measurement of reactive oxygen species (ROS). The production of intracellular ROS was determined using 2,7-dichlorofluorescein diacetate ($DCFH_2$-DA).[14] The $DCFH_2$-DA passively enters the cell, where it reacts with ROS to form the highly fluorescent compound 2,7-dichlorofluorescein. Thus, 10 mM $DCFH_2$-DA stock solution (in methanol) was diluted in culture medium without serum or other additives to yield a 100 μM working solution. At the end of exposure with **2a**, cells were harvested and washed three times with phosphate-buffered saline (PBS). The cell pellet was collected and a homogeneous suspension was made by PBS up to 1 ml. Then, cells were incubated in 1.5 ml working solution of $DCFH_2$-DA at 37 °C for 30 min. Cells were lysed in alkaline solution and centrifuged at 2300 rpm. One milliliter of supernatant was transferred to a cuvette, and fluorescence was measured at 520 nm with a fluorescence spectrophotometer (Hitachi F-1700) using 485 nm excitation. The values were expressed as percent fluorescence intensity relative to control wells (Fig. 5c). Fluorescence micrographs were also taken by phase contrast microscopy. To determine the effective contribution of ROS in **2a**-induced cell death, Jurkat and KG-1A cells were seeded in a 96-well plate at 0.2 ml per well at a concentration of 2×10^5 cells per ml. A stock solution of *N*-acetyl cysteine (NAC) was made with sterile water and added to cells at 10 mM for 1 h.[14] After NAC pretreatment, cells were cultured with compound **2a** for 24 h and after the treatment schedule the cell viability was estimated by the MTT method. Fig. 5d shows that NAC had significant effect in preventing **2a** induced cytotoxicity, with rescue being observed at different concentrations of **2a** tested. Significant differences ($p < 0.05$) were observed between cultures not pretreated with NAC and those pre-treated with NAC (5 mM) for **2a** at all concentrations tested. For example, with 5 mM NAC, nearly 100% viability was retained even at **2a** concentration previously shown to reduce cell viability below 15%. These results indicate that ROS generation plays a pivotal role in **2a**-induced cytotoxicity (Fig. 5d). From our findings it is apparent that compound **2a** exhausted the cellular defense system by generating an excess amount of intracellular ROS. Excessive amounts of ROS can cause oxidative damage to lipids, proteins, and DNA.[15] The observed **2a** induced cytotoxicity has been attributed to uptake of ROS which induced the stress sig-

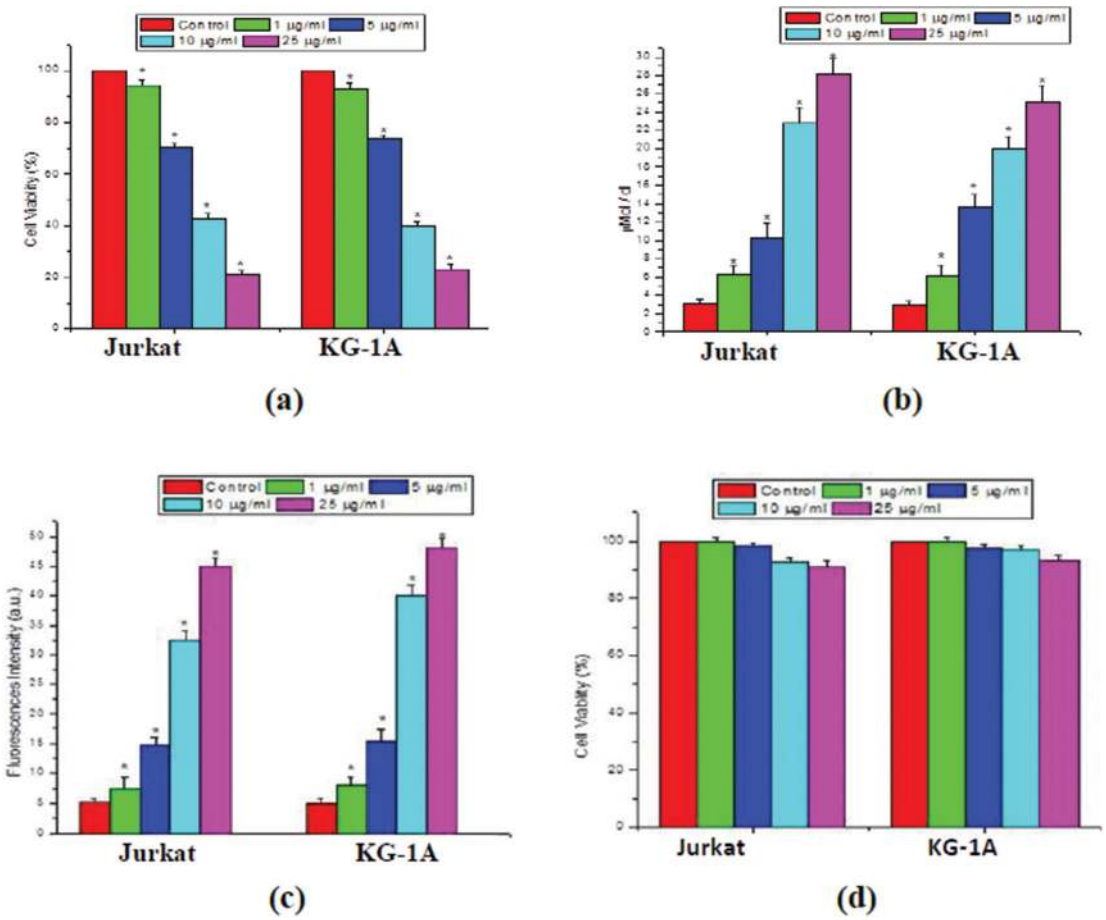

Fig. 5 Estimation of cell viability (a), estimation of LDH activity (b), ROS measurement (c), and role of NAC in cytotoxicity for **2a** with human leukemic cells Jurkat and KG-1A (d).

naling pathway. The application of NAC successfully inhibited the ROS mediated cell damage.

Cell imaging. The fluorescence image of the cells was taken with a phase-contrast fluorescence microscope at 400 magnification.[16] The cellular internalization of compound **2a** is an endocytic process.[17] Compound **2a** binds to the plasma membrane and is internalized into membrane-bound endocytic vesicles which are transported through the cell by motor proteins moving along the cytoskeleton.[18] Fluorescence images (Fig. 6) indicate that compound **2a** was well distributed in the cytoplasm and migrates towards the nucleus. Compound **2a** also preferentially targeted the cancer cells and was internalized. Receptor-mediated endocytosis process may be involved in this internalization.[19]

DNA binding studies. The importance of DNA binding agents is inevitable in cancer biology due to their potential therapeutic use. Small molecules employed as anticancer agents exert their effect by directly acting on DNA. Non-covalent interaction of such natural and synthetic molecules to DNA mostly involves either an intercalative or minor groove binding mechanism. Thus, the study of DNA interaction with this compound is necessary for further development of more effective therapeutic agents. The binding mode and mechanism of interaction to CT DNA were examined with the help of different biophysical techniques.

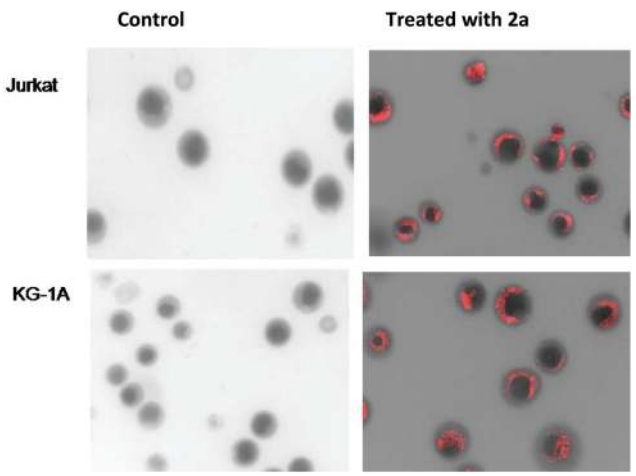

Fig. 6 Cell imaging with **2a** for human leukemic Jurkat and KG-1A cells.

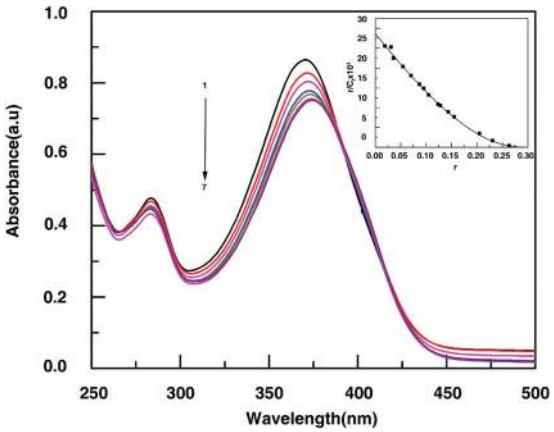

Fig. 7 Absorption spectral changes of compound **2a** (2 μM) treated with 0, 4, 8, 12, 16, 20, and 24 μM (curves 1–7) of CT-DNA. Inset: a fitting of the absorbance data used to obtain the binding constants.

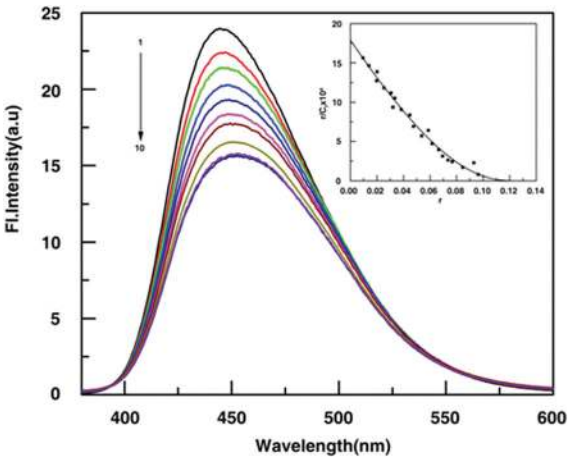

Fig. 8 Fluorescence spectra of compound **2a** (5 μM) (T = 30 °C, λ_{ex} = 370 nm) treated with different concentrations of CT-DNA. In the panel, curves (1–10) denote 0, 10, 20, 30, 40, 50, 60, 70, 80, and 90 μM of compound **2a**. Inset: a fitting of the fluorescence data used to obtain the binding constants.

Absorption spectroscopy and binding affinity evaluation. Interaction of small molecules with DNA can be suitably monitored using electronic spectroscopy by the changes in absorbance and the shift in wavelength maxima. The effect of gradually increasing the concentration of DNA on the absorption spectrum of compound **2a** is depicted in Fig. 7. The characteristic hypochromism, sharp isosbestic points, and saturation at high DNA concentrations suggest a simple two state transition between the free and bound drugs. The absorption spectrum shows the wavelength maximum at 372 and 283 nm with sharp isosbestic points at 389 nm. Since no evidence for any cooperativity (no positive slope at low input values of the drug) was detected, the Scatchard plots were analyzed using the McGhee–von Hippel equation[20] for non-cooperative ligand binding (eqn (1)). The solid lines represent the best fit of the experimental value to eqn (1), where K is the intrinsic binding constant to an isolated binding site, and n is the number of nucleotides occluded by the binding of a single ligand molecule. The results obtained from the experiment confirmed that the CT-DNA binding to the compound is non-cooperative. The binding affinity (K) of **2a** with DNA is 1.20×10^5 M^{-1} with exclusion sites (n) of 4.68 base pairs.

$$r/C_f = K(1 - nr)[(1 - nr)/\{1 - (n - 1)r\}]^{(n-1)} \quad (1)$$

Fluorescence spectroscopy and binding affinity evaluation. The synthesized compound **2a** is highly fluorescent with emission spectra in the range of 400–600 nm when excited at 370 nm with a maximum at 444 nm. Binding to CT DNA quenches the fluorescence intensity of **2a** with a red shift of 8 nm indicative of strong association (Fig. 8). The binding constants (K) and the number of excluded sites (n) for the interaction were estimated from the fits to the non-cooperative equation of McGhee–von Hippel (eqn (1)).[20] The binding affinity (K) of compound **2a** with DNA is 1.79×10^5 M^{-1} with exclusion sites (n) of 5.10 base pairs.

Isothermal titration calorimetry. Small molecule binding to macromolecules can also be conveniently examined by using isothermal titration calorimetry (ITC).[21] The use of ITC is advantageous because it offers the complete thermodynamic profile of the binding. The Gibbs free energy (ΔG), enthalpy change (ΔH), and entropy change and the estimation of the binding affinity (K) and the stoichiometry (n) can be obtained in a single experiment. The representative ITC profile of the binding is shown in Fig. 9. In the upper panel the representative raw ITC profiles resulting from the titration of compound **2a** binding to the CT DNA under study are depicted. It can be seen that the binding of the compound to DNA provided ITC thermograms consistent with exothermic binding and showed a single exothermic event. The calorimetric data were fitted to a single set of identical sited models yielding $\Delta H = -0.487 \pm 0.02$ kcal mol^{-1}, a stoichiometry (N) of 0.342 and $K = (2.99 \pm 0.48) \times 10^5$ M^{-1} and the entropy contribution ($T\Delta S$) = 6.98 kcal mol^{-1} for CT-DNA. For intercalators, the magnitude of the binding enthalpy is large and negative. Considering the significant changes in entropy, the association of compound **2a** to CT-DNA seems to be entropy driven. These values are similar to those observed for other groove binders.[22] Thus, compound **2a** may also be a groove binder.

Conclusions

A novel class of bridgehead polycyclic nitrogen heterocycles, pyrido[1,2-*a*]pyrimidinium ions, has been introduced. They could be easily prepared *via* a two step one-pot reaction from readily available starting materials. They are bench stable ionic compounds with highly fluorescent properties. Such characteristics enable us to explore their biological activities with human leukemic cells Jurkat and KG-1A. Our findings from

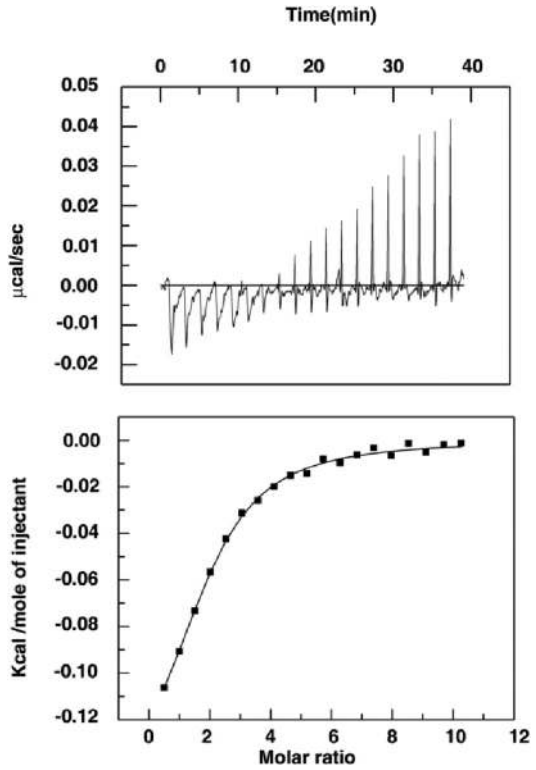

Fig. 9 ITC profiles for the binding of compound **2a** to CT-DNA. Top panels present raw results for the sequential injection of aliquots of CT-DNA (1000 μM); 2 μL each were injected into the isothermal sample chamber containing compound **2a** (20 μM) in citrate–phosphate buffer (pH 7.10) at 25 °C. The bottom panels show the integrated heat results after correction of the heat of dilution against the mole ratio. The data points were fitted to the one site model and the solid lines represent the best-fit data.

DNA interaction, cell imaging, and cell viability experiments demonstrate that this new class of compounds could be a potential candidate for cancer diagnosis.

Experimental section

General information

^{1}H NMR (300 MHz) and ^{1}H NMR (400 MHz) spectra were recorded on a 300 MHz and a 400 MHz spectrometer in $CDCl_3$/DMSO-d_6 solvent using TMS as the internal standard. HRMS was measured using a TOF analyzer. Chromatographic purification was done with either 60–120 or 100–200 mesh silica gel (SRL). For reaction monitoring, precoated silica gel 60 F254 TLC sheets (Merck) were used. Petroleum ether refers to the fraction boiling in the range 60–80 °C. Solvents were dried, distilled and stored over molecular sieves (4 Å). 3-(4,5-Dimethylthiazol)-2-diphenyltetrazolium bromide (MTT reagent), Histopaque 1077, two human leukemic cells Jurkat and KG-1A, and *N*-acetyl cysteine were procured from Sigma (St. Louis, MO, USA). RPMI 1640, fetal bovine serum (FBS), penicillin, streptomycin, sodium chloride (Nacl), sodium carbonate (Na_2CO_3), sucrose, and Hanks balanced salt solution were purchased from Himedia (Mumbai, India).

Materials and methods

The cellular internalization of compound **2a** on KG-1A and Jurkat was performed *in vitro* by drug uptake assay using fluorescence microscopic imaging. Briefly, Rhodamine B (Rh-B) labeled compound **2a** was prepared through the following process. Ten μg ml^{-1} Compound **2a** was dissolved in water and conjugated with 25 μl of Rh-B (1 mg ml^{-1}). This mixture was stirred for 24 hours at 37 °C using a magnetic stirrer (REMI, India). Then, the fluoro-labeled **2a** was separated by centrifugation at 4 °C. The obtained sediment was washed with deionized water and re-dispersed. This process was repeated three times to remove the un-reacted Rh-B. Finally, the obtained Rh-B labeled compound **2a** (Rh-B-compound **2a**) was dispersed in culture medium for *in vitro* experiment.

KG-1A and Jurkat cells were plated at a density of 2×10^4 cells per μl in Petridish (35 mm) for 24 h. Rh-B tagged compound **2a** at 25 μg ml^{-1} dose was incubated for 6 hours at 37 °C under a 95% air/5% CO_2 atmosphere in a CO_2 incubator. After the defined time, the coverslips were removed and the cells were washed 2 times with PBS (50 mM) and immediately observed in green light under a fluorescence microscope (NIKON ECLIPSE LV100POL) for uptake study. Images were acquired at 400× optical zoom and analysis was done using ImageJ software v.r.1.43 (NIH).[23]

A Shimadzu Pharmaspec1700 unit (Shimadzu Corporation, Kyoto, Japan) was used for absorption spectral studies. For this purpose a constant concentration of compound **2a** was treated with increasing concentration of CT-DNA in one cm path length matched quartz cells with continuous stirring. The amount of free and bound drugs was determined as described previously.[24,25]

Fluorescence spectral studies were performed using a Hitachi F7000 (Hitachi Ltd, Tokyo, Japan). The excitation wavelength for the compound was 370 nm and all measurements were performed keeping an excitation and emission band-pass of 2.5 nm. Binding data obtained from spectrophotometric and spectrofluorometric titrations of increasing concentrations of DNA to a fixed concentration of the compound were transmitted into the form of a Scatchard plot of r/C_f *versus* r, where r is the number of compound **2a** bound per mole of DNA base pairs. Non-linear binding isotherms observed were fitted to a theoretical curve drawn according to the excluded site model of McGhee and von Hippel[20] for a non-cooperative ligand binding system using the following equation:

$$r/C_f = K(1 - nr)[(1 - nr)/\{1 - (n - 1)r\}]^{(n-1)} \quad (1)$$

where K is the intrinsic binding constant to an isolated binding site, and n is the number of nucleotides occluded by the binding of a single ligand molecule.

Isothermal titration calorimetry (ITC) experiments were performed on a GE Microcal ITC 200 (Northampton, USA) microcalorimeter. Origin 7.0 software was used for data acquisition

and manipulation. In a typical experiment aliquots of degassed DNA solution were injected from a rotating syringe (750 rpm) into the isothermal sample chamber containing the complex solution. Corresponding control experiments to determine the heat of dilution of DNA were performed by injecting identical volumes of DNA into the buffer. The volume of the injection was 2 μl and the duration of each injection was 4 s, and the delay time between each injection was 120 s. The initial delay before the first injection was 60 s. Each injection generated a heat burst curve (microcalories per second *versus* time). The area under each heat burst curve was determined by integration using the Origin 7.0 software (MicroCal) to give a measure of the heat associated with that injection. The heat associated with each DNA-buffer mixing was subtracted from the corresponding heat associated with the DNA injection to the complex to give the heat of the complex binding to DNA. The heat of dilution of injecting the buffer into the complex solution was observed to be negligible. The resulting corrected injection heats were plotted as a function of the [compound]/[molar ratio], fit with a model for one set of binding sites, and analyzed using Origin 7.0 software to estimate the binding affinity (K_b), the binding stoichiometry (N) and the enthalpy of binding (ΔH). The free energies (ΔG) were calculated using the standard equation:

$$\Delta G = -RT \ln(K_b) \quad (2)$$

where R is 1.987 cal mol^{-1}, and K and T are represented in units of Kelvin for the appropriate temperature. The binding free energy coupled with the binding enthalpies derived from the ITC data allowed the calculation of the entropic contribution to the binding ($T\Delta S$), where $T\Delta S$ is the calculated binding entropy using the standard relationship

$$T\Delta S = \Delta H - \Delta G \quad (3)$$

General procedure for the synthesis of pyrido[1,2-a]-pyrimidinium ions

Compound **1** (1.0 mmol) and 2-aminopyridine (1.1 mmol) were placed in a round bottomed flask. Methanol (3 ml) was added followed by a drop of acetic acid catalyst. The reaction mixture was allowed to reflux and the progress of the reaction was monitored by TLC. After the disappearance of the starting material (8 h), the reaction mixture was evaporated to dryness with the addition of silica gel. The crude product was purified by column chromatography on Silica Gel (60–120) with the eluent dichloromethane and methanol (20 : 1).

Characterization data of compounds (2a–2s)

10-Methoxy-7,8-dihydrobenzo[*h*]pyrido[1,2-*a*]quinazolin-13-ium bromide (2a). Yellow solid; mp 130 °C; ^{1}H NMR (300 MHz, $CDCl_3$) δ: 2.86–2.99 (m, 4H), 3.85 (s, 3H), 6.74–6.83 (m, 2H), 7.13–7.17 (m, 1H), 7.24–7.26 (m, 1H), 7.70–7.79 (m, 2H), 8.50–8.53 (m, 1H), 9.40 (s, 1H); ^{13}C NMR (75 MHz, $CDCl_3$) δ: 24.7, 27.7, 55.4, 111.7, 113.3, 119.2, 121.6, 127.0, 130.1, 132.9, 134.0, 135.7, 136.9, 140.6, 149.0, 161.0, 163.8; HRMS Calcd for $C_{17}H_{15}N_2O$ $[M]^+$ 263.1179; found 263.1176.

7,8-Dihydrobenzo[*h*]pyrido[1,2-*a*]quinazolin-13-ium bromide (2b). Yellow solid; mp 170–172 °C; ^{1}H NMR (400 MHz, DMSO-d_6) δ: 3.00–3.09 (m, 4H), 7.52–7.60 (m, 2H), 7.66–7.73 (m, 2H), 8.04–8.10 (m, 1H), 8.50–8.62 (m, 2H), 9.11–9.13 (m, 1H), 9.42 (s, 1H); ^{13}C NMR (100 MHz, DMSO-d_6) δ: 24.7, 27.0, 113.8, 124.0, 125.2, 127.4, 129.6, 133.7, 134.3, 135.0, 136.7, 140.6, 141.5, 149.6, 154.4, 161.9; HRMS Calcd for $C_{16}H_{13}N_2[M]^+$: 233.1073; found 233.1074.

9-Methoxy-7,8-dihydrobenzo[*h*]pyrido[1,2-*a*]quinazolin-13-ium bromide (2c). Yellow solid; mp 145 °C: ^{1}H NMR (400 MHz, DMSO-d_6) δ: 2.95–3.06 (m, 2H), 3.10–3.24 (m, 2H), 3.94 (s, 3H), 7.36–7.48 (m, 1H), 7.53–7.57 (m, 1H), 8.02–8.13 (m, 2H), 8.34–8.56 (m, 2H), 9.08–9.11 (m, 1H), 9.42 (s, 1H); ^{13}C NMR (100 MHz, DMSO-d_6,) δ: 22.5, 26.1, 51.8, 109.2, 113.7, 122.9, 125.0, 127.3, 129.4, 132.1, 133.7, 134.1, 134.8, 139.8, 141.0, 149.5, 160.2; HRMS Calcd for $C_{17}H_{15}N_2O$ $[M]^+$: 263.1179; found 263.1175.

11-Methoxy-7,8-dihydrobenzo[*h*]pyrido[1,2-*a*]quinazolin-13-ium bromide (2d). Yellow solid; mp 135 °C; ^{1}H NMR (300 MHz, $CDCl_3$) δ: 2.86–3.01 (m, 2H), 3.11–3.15 (m, 2H), 3.98 (s, 3H), 6.64–6.68 (m, 1H), 6.73–6.76 (m, 1H), 7.23–7.36 (m, 2H), 8.02–8.03 (m, 1H), 8.51–8.52 (m, 2H), 9.31 (s, 1H); ^{13}C NMR (75 MHz, $CDCl_3$) δ: 25.5, 26.5, 55.7, 110.9, 112.2, 119.9, 122.6, 124.5, 127.0, 129.2, 130.7, 133.4, 134.2, 136.8, 138.8, 140.6, 159.5; HRMS Calcd for $C_{17}H_{15}N_2O$ $[M]^+$: 263.1179; found 263.1178.

11-Nitro-7,8-dihydrobenzo[*h*]pyrido[1,2-*a*]quinazolin-13-ium bromide (2e). Yellow solid; mp 180 °C; ^{1}H NMR ($CDCl_3$, 300 MHz) δ: 2.95–3.02 (m, 4H), 7.21–7.31 (m, 2H), 7.34–7.40 (m, 1H), 7.74–7.77 (m, 1H), 8.13–8.17 (m, 1H), 8.20–8.26 (m, 1H), 8.69–8.70 (m, 1H), 9.43 (s, 1H); ^{13}C NMR ($CDCl_3$, 75 MHz) δ: 23.5, 31.4, 109.9, 113.3, 114.0, 123.5, 124.9, 128.3, 134.5, 135.5, 139.2, 144.8, 145.6, 147.4, 149.1, 157.9; HRMS Calcd for $C_{16}H_{12}N_3O_2$ $[M]^+$: 278.0924; found 278.0923.

7,8,9,10,11,12-Hexahydrocycloocta[*e*]pyrido[1,2-*a*]pyrimidin-13-ium bromide (2f). Yellow liquid; ^{1}H NMR (300 MHz, $CDCl_3$) δ: 1.25–1.34 (m, 4H), 1.89–2.03 (m, 4H), 2.78–2.88 (m, 4H), 8.22–8.29 (m, 2H), 8.38–8.42 (m, 1H), 9.61–9.64 (d, 1H, J = 6.0 Hz), 10.15 (s, 1H); ^{13}C NMR (75 MHz, $CDCl_3$) δ: 25.7, 28.3, 29.7, 30.9, 35.4, 39.7, 113.0, 121.5, 126.4, 134.0, 137.3, 140.0, 152.8, 164.2. HRMS Calcd for $C_{14}H_{17}N_2$ $[M]^+$: 213.1386; found 213.1387.

8,9,10,11-Tetrahydro-7*H*-cyclohepta[*e*]pyrido[1,2-*a*]pyrimidin-12-ium bromide (2g). Yellow liquid; ^{1}H NMR (300 MHz, $CDCl_3$) δ: 1.82–1.94 (m, 4H), 1.95–2.05 (m, 2H), 3.12–3.19 (m, 4H), 7.79–7.82 (m, 1H), 8.31–8.39 (m, 2H), 9.55–9.60 (m, 1H), 9.81 (s, 1H);^{13}C NMR (75 MHz, $CDCl_3$) δ: 25.2, 25.8, 31.6 (2C), 40.3, 112.4, 123.6, 126.9, 135.7, 136.1, 139.5, 146.5, 156.5. HRMS Calcd for $C_{13}H_{15}N_2$ $[M]^+$: 199.1230; found 199.1231.

2-Chloro-7,8-dihydrobenzo[*h*]pyrido[1,2-*a*]quinazolin-13-ium bromide (2h). Yellow solid; mp 183–185 °C; ^{1}H NMR (300 MHz, $CDCl_3$) δ: 2.74–2.79 (m, 2H), 2.94–2.98 (m, 2H), 6.75–6.78 (m, 1H), 7.39–7.46 (m, 1H), 7.55–7.58 (m, 2H), 8.01–8.12 (m, 2H), 8.62 (s, 1H), 9.73 (s, 1H); ^{13}C NMR (75 MHz,

$CDCl_3$) δ: 28.0, 29.7, 107.9, 112.1, 124.8, 126.9, 127.6, 132.4, 134.7, 138.0, 139.1, 140.7, 142.5, 146.9, 150.6, 163.3; HRMS Calcd for $C_{16}H_{12}ClN_2$ $[M]^+$: 267.0684; found 267.0683.

2-Chloro-11-methoxy-7,8-dihydrobenzo[*h*]pyrido[1,2-*a*]quinazolin-13-ium bromide (2i). Yellow solid; mp 218 °C; ^{1}H NMR (300 MHz, DMSO-d_6) δ: 2.89–2.94 (m, 2H), 3.07–3.10 (m, 2H), 3.90 (s, 3H), 7.31–7.35 (m, 1H), 7.47–7.50 (m, 1H), 7.66–7.67 (m, 1H), 8.52–8.55 (m, 1H), 8.70–8.73 (m, 1H), 9.44 (s, 1H), 9.56 (s, 1H); ^{13}C NMR (75 MHz, DMSO-d_6) δ: 25.4, 26.0, 56.1, 110.9, 112.7, 122.0, 125.7, 128.6, 129.5, 131.0, 134.5, 135.3, 139.9, 141.5, 147.3, 148.5, 159.4; HRMS Calcd for $C_{17}H_{14}ClN_2O$ $[M]^+$: 297.0789; found 297.0788.

2-Chloro-10-methoxy-7,8-dihydrobenzo[*h*]pyrido[1,2-*a*]quinazolin-13-ium bromide (2j). Yellow solid; mp 222 °C; ^{1}H NMR (300 MHz, DMSO-d_6) δ: 2.87–2.97 (m, 2H), 3.09–3.11 (m, 2H), 3.93 (s, 3H), 7.13–7.21 (m, 2H), 7.26 (s, 1H), 8.52–8.68 (m, 2H), 9.40 (s, 1H), 9.65 (s, 1H); ^{13}C NMR (75 MHz, DMSO-d_6) δ: 24.9, 27.2, 56.4, 113.6, 115.3, 118.2, 130.1, 131.2, 132.4, 134.8, 139.3, 142.0, 143, 146.9, 148.7, 155.0, 162.5; HRMS Calcd for $C_{17}H_{14}ClN_2O$ $[M]^+$: 297.0789; found 297.0788.

2-Chloro-8-methyl-7,8-dihydrobenzo[*h*]pyrido[1,2-*a*]quinazolin-13-ium bromide (2k). Yellow liquid; ^{1}H NMR (300 MHz, DMSO-d_6) δ: 1.22 (d, 3H, J = 6.0 Hz), 2.48–2.49 (m, 2H), 3.10–3.16 (m, 1H), 7.55–7.60 (m, 2H), 7.71–7.76 (m, 1H), 8.47–8.52 (m, 2H), 8.64–8.67 (m, 1H), 9.35 (s, 1H), 9.50 (s, 1H); ^{13}C NMR (75 MHz, DMSO-d_6,) δ: 21.5, 31.2, 31.7, 127.7, 128.3, 128.6 (2C), 128.7, 129.0, 129.7, 134.5, 135.5, 140.6, 141.7, 147.4, 147.9, 161.7; HRMS Calcd for $C_{17}H_{14}ClN_2$ $[M]^+$: 281.0840; found 281.0841.

2-Chloro-7,8,9,10-tetrahydropyrido[1,2-*a*]quinazolin-11-ium bromide (2l). Yellow liquid; ^{1}H NMR (300 MHz, DMSO-d_6) δ: 1.87–1.90 (m, 4H), 2.65–2.76 (m, 4H), 8.35–8.38 (m, 1H), 8.54–8.58 (m, 1H), 9.26 (s, 1H), 9.38 (s, 1H); ^{13}C NMR (75 MHz, DMSO-d_6) δ: 20.8, 24.4, 26.6, 30.9, 127.4, 128.4, 130.0, 133.9, 139.8, 141.2, 146.1, 163.4; HRMS Calcd for $C_{12}H_{12}ClN_2$ $[M]^+$: 219.0684; found: 219.0685.

2-Chloro-7,8,9,10,11,12-hexahydrocycloocta[*e*]pyrido[1,2-*a*]-pyrimidin-13-ium bromide (2m). Yellow liquid; ^{1}H NMR (300 MHz, $CDCl_3$) δ: 1.21–1.26 (m, 2H), 1.60–1.81 (m, 6H), 2.79–2.95 (m, 4H), 8.18–8.25 (m, 1H), 8.29–8.40 (m, 1H), 9.68 (s, 1H), 10.08 (s, 1H); ^{13}C NMR (75 MHz, $CDCl_3$) δ: 25.6 (2C), 29.0, 30.6, 31.4, 35.4, 127.3, 131.4, 134.2, 135.5, 140.9, 141.3, 145.4, 166.5. HRMS Calcd for $C_{14}H_{16}ClN_2$ $[M]^+$: 247.0997; found: 247.0998.

9-Methoxy-4-methyl-7,8-dihydrobenzo[*h*]pyrido[1,2-*a*]quinazolin-13-ium bromide (2n). Yellow solid, mp 165 °C; ^{1}H NMR (300 MHz, $CDCl_3$) δ: 2.89–2.94 (m, 4H), 3.86 (s, 6H), 6.90–6.98 (m, 1H), 7.05–7.10 (m, 1H), 7.22–7.30 (m, 1H), 7.51–7.55 (m, 2H), 8.32–8.34 (m, 1H), 9.40 (s, 1H): ^{13}C NMR (75 MHz, $CDCl_3$) δ: 24.0, 27.3, 54.1, 56.7, 109.3, 112.8, 118.0, 119.9, 125.8, 126.1, 128.0, 132.1, 134.7, 135.4, 139.7, 143.8, 152.5, 162.4; HRMS Calcd for $C_{18}H_{17}N_2O$ $[M]^+$: 277.1335; found: 277.1334.

9-Methoxy-1-methyl-7,8-dihydrobenzo[*h*]pyrido[1,2-*a*]quinazolin-13-ium bromide (2o). Yellow solid; mp 171 °C; ^{1}H NMR (300 MHz, $CDCl_3$) δ: 2.83–2.93 (m, 4H), 3.90 (s, 6H), 6.94–6.99 (m, 1H), 7.25–7.31 (m, 2H), 7.51–7.55 (m, 1H), 7.62–7.69 (m, 1H), 8.14–8.17 (m, 1H), 9.30 (s, 1H).^{13}C NMR (75 MHz, $CDCl_3$) δ: 22.0, 25.2, 56.1 (2C), 111.1, 114.2, 115.0, 118.3, 126.3, 130.2, 132.6, 135.8, 139.1, 140.0, 143.2, 144.1, 148.4, 165.1; HRMS Calcd for $C_{18}H_{17}N_2O$ $[M]^+$: 277.1335; found 277.1336.

10-Methoxy-2-methyl-7,8-dihydrobenzo[*h*]pyrido[1,2-*a*]quinazolin-13-ium bromide (2p). Yellow solid, mp 149 °C; ^{1}H NMR (300 MHz, $CDCl_3$) δ: 2.89–3.11 (m, 4H), 3.90 (s, 3H), 3.93 (s, 3H), 7.08–7.15 (m, 2H), 7.24–7.29 (m, 1H), 7.72 (s, 1H), 7.89–7.92 (m, 1H), 8.09–8.12 (m, 1H), 9.32 (s, 1H);^{13}C NMR (75 MHz, $CDCl_3$) δ: 21.5, 24.7, 56.3 (2C), 109.2, 113.3, 120.7, 125.3, 126.4, 128.2, 130.7, 131.4, 134.4, 139.8, 143.5, 148.4, 157.3, 164.6; HRMS Calcd for $C_{18}H_{17}N_2O$ $[M]^+$: 277.1335; found 277.1338.

2,8-Dimethyl-7,8-dihydrobenzo[*h*]pyrido[1,2-*a*]quinazolin-13-ium bromide (2q). Yellow liquid; ^{1}H NMR (300 MHz, DMSO-d_6) δ: 1.23 (d, 3H, J = 6.0 Hz), 2.59 (s, 2H), 3.07–3.12 (m, 1H), 3.32 (s, 3H), 7.53–7.56 (m, 2H), 7.67–7.72 (m, 1H), 8.36–8.41 (m, 2H), 8.45–8.47 (m, 1H), 8.98 (s, 1H), 9.35 (s, 1H); ^{13}C NMR (75 MHz, DMSO-d_6) δ: 18.3, 21.4, 31.3, 31.8, 126.8, 127.4, 127.6, 128.5 (2C), 129.3, 134.2 (2C), 135.0, 140.4, 143.6, 147.2, 147.5, 160.8; HRMS Calcd for $C_{18}H_{17}N_2$ $[M]^+$: 261.1386; found 261.1387.

2-Methyl-7,8,9,10-tetrahydropyrido[1,2-*a*]quinazolin-11-ium bromide (2r). Yellow liquid; ^{1}H NMR (300 MHz, DMSO-d_6,) δ: 2.49–2.55 (m, 4H), 2.71–2.73 (m, 4H), 3.31 (s, 3H), 7.92 (s, 1H), 8.25–8.36 (m, 1H), 8.87 (s, 1H), 9.26 (s, 1H); ^{13}C NMR (75 MHz, DMSO-d_6) δ: 18.3, 22.2, 24.4, 26.6, 37.0, 126.6, 129.3, 133.8, 138.5, 141.0, 143.1, 145.9, 162.4. HRMS Calcd for $C_{13}H_{15}N_2$ $[M]^+$: 199.1230; found 199.1231.

2-Methyl-7,8,9,10,11,12-hexahydrocycloocta[*e*]pyrido[1,2-*a*]-pyrimidin-13-ium bromide (2s). Yellow liquid; ^{1}H NMR (300 MHz, $CDCl_3$) δ: 1.47–1.64 (m, 4H), 1.91–2.05 (m, 5H), 2.62–2.73 (m, 3H), 3.36 (s, 3H), 7.71–7.79 (m, 1H), 8.05–8.11 (m, 1H), 9.38 (s, 1H), 9.89 (s, 1H); ^{13}C NMR (75 MHz, $CDCl_3$) δ: 17.3, 26.4, 27.3, 28.0, 31.6, 37.0, 55.2, 107.7, 109.3, 125.8, 136.9, 139.6, 140.0, 145.2, 164.4; HRMS Calcd for $C_{15}H_{19}N_2$[M]$^+$: 227.1543; found 227.1544.

Acknowledgements

The financial support from DST (no. SB/FT/CS-189/2012), UGC-MRP (no. PSW-086/11-12), UGC (New Delhi) [NO.F. 20 7(17)/2012(BSR)] and the Chemistry Department of Haldia Govt. College is gratefully acknowledged. Special thanks are due to Suhitananda Maharaj for constant inspiration. SKM also thank Dr. B. Ghosh for crystallographic discussion.

Notes and references

1 (*a*) J. A. Joule and K. Mills, *Heterocyclic Chemistry*, Blackwell, Oxford, UK, 4th edn, 2000; (*b*) *Comprehensive Heterocyclic Chemistry: The Structure, Reactions, Synthesis, and Uses of Heterocyclic Compounds*, ed. A. R. Katrizky and C. W. Rees, Pergamon Press, Oxford, UK, 1984, vol. 1–8; (*c*) H. Fan,

J. Peng, M. T. Hamann and J.-F. Hu, *Chem. Rev.*, 2008, **108**, 264.

2 (*a*) J. F. Swinbourne, H. J. Hunt and G. Klinkert, *Adv. Heterocycl. Chem.*, 1987, **23**, 103; (*b*) I. Hermecz and Z. Mészáros, *Med. Res. Rev.*, 1988, **8**, 203; (*c*) G. Doria, C. Passarotti, R. Magrini, A. Forgione, P. Sberze, M. T. M. L. Corno, G. Cruzzola and G. Cadelli, *Eur. J. Med. Chem.*, 1983, **18**, 227; (*d*) C. Devos, F. Dessy, I. Hermecz, Z. Meszaros and T. Breining, *Int. Arch. Allergy Immunol.*, 1982, **67**, 362.

3 I. Hermecz, L. Vasvari-Debreczy and P. Matyus, in *Comprehensive Heterocyclic Chemistry*, ed. A. R. Katritzky, C. W. Rees and E. V. F. Scriven, Pergamon, London, 1996, ch. 8.23, pp. 563–595, and references cited therein.

4 C. O. Kappe and T. Kappe, *Arch. Pharm.*, 1991, **324**, 863.

5 P. Lennig, S. Stengelin, T. Klabunde, M. Gossel, P. Safar, M. Smrcina, J. Spoonamore, G. Merriman, J. T. Klein, B. Whiteley, C. Lanter; K. Bordeau and Z. Yang, *PCT Int. Appl*, WO2006,24390, 2006; *Chem. Abstr.*, 2006, **144**, 274545g.

6 (*a*) A. R. Katritzky, J. W. Rogers, R. M. Witek and S. K. Nair, *ARKIVOC*, 2004, (viii), 52; (*b*) J. Zeng, Y. J. Tan, M. L. Leow and X.-W. Liu, *Org. Lett.*, 2012, **14**, 4386; (*c*) H. Cao, X. Liu, L. Zhao, J. Cen, J. Lin, Q. Zhu and M. Fu, *Org. Lett.*, 2014, **16**, 146; (*d*) A. L. Rousseau, P. Matlaba and C. J. Parkinson, *Tetrahedron Lett.*, 2007, **48**, 4079; (*e*) N. Chernyak and V. Gevorgyan, *Angew. Chem., Int. Ed.*, 2010, **49**, 2743; (*f*) L. Ma, X. Wang, W. Yu and B. Han, *Chem. Commun.*, 2011, **47**, 11333; (*g*) M. J. Corr, M. D. Roydhouse, K. F. Gibson, S.-z. Zhou, A. R. Kennedy and J. A. Murphy, *J. Am. Chem. Soc.*, 2009, **131**, 17980.

7 (*a*) F. C. Colpaert, *Nat. Rev. Drug Discovery*, 2003, **2**, 315; (*b*) G. Leoncini, M. G. Signorello, G. Roma and M. D. Braccio, *Biochem. Pharmacol.*, 1997, **53**, 1667; (*c*) V. S. Bogdanov, K. L. Cherkasova, V. A. Dorokhov, O. V. Shishkin and Y. T. Struchkov, *Mendeleev Commun.*, 1995, **5**, 106; (*d*) M. Güllü, S. Uzun and S. Yalcin, *Tetrahedron Lett.*, 2003, **44**, 1939; (*e*) B. Djerrari, E. M. Essassi, J. Fifani and B. Garrigues, *C. R. Chim.*, 2002, **5**, 177; (*f*) J. M. Mellor, G. D. Merriman, H. Rataj and G. Reid, *Tetrahedron Lett.*, 1996, **37**, 2615.

8 (*a*) M. Adib, H. Yavari and M. Mollahosseini, *Tetrahedron Lett.*, 2004, **45**, 1803; (*b*) M. Adib, M. H. Sayahi, M. Nosratia and L.-G. Zhu, *Tetrahedron Lett.*, 2007, **48**, 4195; (*c*) D. Cheng, L. Croft, M. Abdi, A. Lightfoot and T. Gallagher, *Org. Lett.*, 2007, **9**, 5175.

9 (*a*) S. K. Manna, S. K. Mondal, A. Ahmed, A. Mandal, A. Jana, M. Ikbal, S. Samanta and J. K. Ray, *RSC Adv.*, 2014, **4**, 2474; (*b*) S. K. Mondal, S. K. Manna, A. Mandal, S. Samanta and J. K. Ray, *Tetrahedron Lett.*, 2014, **55**, 6411.

10 (*a*) K. Toshima, R. Takano, T. Ozawa and S. Matsumura, *Chem. Commun.*, 2002, 212; (*b*) S. v. d. Steen, P. d. Hoog, K. v. d. Schilden, P. Gamez, M. Pitié, R. Kissc and J. Reedijk, *Chem. Commun.*, 2010, **46**, 3568.

11 (*a*) M. J. Waring, *Annu. Rev. Biochem.*, 1981, **50**, 159; (*b*) L. H. Hurley, *Biochem. Soc. Trans.*, 2001, **29**, 692; (*c*) L. H. Hurley, *Nat. Rev. Cancer*, 2002, **2**, 188; (*d*) R. Martinez and L. Chacon-Garcia, *Curr. Med. Chem.*, 2005, **12**, 127; (*e*) R. Palchaudhuri and P. J. Hergenrother, *Curr. Opin. Biotechnol.*, 2007, **18**, 497; (*f*) M. Maiti and G. Suresh Kumar, *Med. Res. Rev.*, 2007, **27**, 649.

12 S. Brahma and J. K. Ray, *Tetrahedron*, 2008, **64**, 288.

13 S. Chattopadhyaya, S. K. Dash, S. Tripathy, B. Das, S. K. Mahapatra, P. Pramanikc and S. Roy, *J. Appl. Toxicol.*, 2015, 1, DOI: 10.1002/jat.3080.

14 C. Hanley, J. Layne, A. Punnoose, K. M. Reddy, I. Coombs, A. Coombs, K. Feris and D. Wingett, *Nanotechnology*, 2008, **19**, 295103.

15 (*a*) G. Perry, *Free Radicals Biol. Med.*, 2000, **28**, 831; (*b*) S. Lanone, F. Rogerieux, J. Geys, A. Dupont, E. M. Marechal, J. Boczkowski, G. Lacroix and P. Hoet, *Part. Fibre Toxicol.*, 2009, **6**, 14.

16 S. K. Sahu, A. Chakrabarty, D. Bhattacharya, S. K. Ghosh and P. Pramanik, *J. Nanopart Res.*, 2011, **13**, 2475.

17 A. Gojova, B. Guo, R. S. Kota, J. C. Rutledge, I. M. Kennedy and A. I. Barakat, *Environ Health Perspect.*, 2007, **155**, 403.

18 M. Tagawa, R. Yumoto, K. Oda, J. Nagai and M. Takano, *Drug Metab. Pharmacokinet.*, 2008, **23**, 318.

19 (*a*) S. Mohapatra, S. K. Mallick, T. K. Maiti, S. K. Ghosh and P. Pramanik, *Nanotechnology*, 2007, **18**, 385102; (*b*) K. T. Wilson, S. Fu, K. S. Ramanujam and S. J. Melzer, *Cancer Res.*, 1998, **58**, 2929; (*c*) K. Peters, R. E. Unger, A. M. Gatti, E. Sabbioni, R. Tsaryk and C. Kirkpatrick, *Int. J. Immunopathol. Pharmacol.*, 2007, **20**, 685.

20 J. D. McGhee and P. H. von Hippel, *J. Mol. Biol.*, 1974, **86**, 469.

21 (*a*) N. j. Buurma and i. Haq, *J. Mol. Biol.*, 2008, **381**, 607; (*b*) K. M. Guthrie, A. D. Parenty, L. V. Smith, L. Cronin and A. Cooper, *Biophys. Chem.*, 2007, **126**, 117; (*c*) Y. Liang, *J. Iran. Chem. Soc.*, 2006, **3**, 209; (*d*) A. A. Saboury, *J. Iran. Chem. Soc.*, 2006, **3**, 209; (*e*) I. Haq, *Arch. Biochem. Biophys.*, 2002, **403**, 1; (*f*) R. O'Brien and I. Haq, in *Biocalorimetry 2*, ed. J. E. Ladbury and M. Doyle, John Wiley and Sons Ltd, West Sussex, 2004.

22 J. B. Chaires, *Biopolymers*, 1997, **44**, 201.

23 S. K. Dash, S. S. Dash, S. Chattopadhyay, T. Ghosh, S. Tripathy, S. K. Mahapatra, B. G. Bag, D. Das and S. Roy, *RSC Adv.*, 2015, **5**, 24144.

24 J. B. Chaires, N. Dattagupta and D. M. Crothers, *Biochemistry*, 1982, **21**, 3933.

25 K. Bhadra, M. Maiti and G. S. Kumar, *Biochim. Biophys. Acta*, 2007, **1770**, 1071.